UIC

University of Illinois at Chicago

Department of Mechanical Engineering

Technical Report # MBS00-6-UIC
Department of Mechanical Engineering
University of Illinois at Chicago

October 2000

A LARGE DEFORMATION PLATE ELEMENT FOR MULTIBODY APPLICATIONS

Aki M. Mikkola
Department of Mechanical Engineering
Lappeenranta University of Technology
Skinnarilankatu 34, 53851 Lappeenranta, Finland

Ahmed A. Shabana
Department of Mechanical Engineering
University of Illinois at Chicago
842 West Taylor Street
Chicago, Illinois 60607

This study was supported by the Academy of Finland and, in part, by the National Science Foundation and the U.S. Army Research Office, Research Triangle Park, N.C.

REPORT DOCUMENTATION PAGE

Form Approved
OMB NO. 0704-0188

1. AGENCY USE ONLY (Leave Blank)	2. REPORT DATE October 2000	3. REPORT TYPE AND DATES COVERED Technical Report

4. TITLE AND SUBTITLE
A Large Deformation Plate Element for Multibody Applications

5. FUNDING NUMBERS
DAAG55-97-1-0303

6. AUTHOR(S)
Aki M. Mikkola and Ahmed A. Shabana

7. PERFORMING ORGANIZATION NAME(S) AND ADDRESS(ES)
University of Illinois- Chicago
Chicago, IL 60607

8. PERFORMING ORGANIZATION REPORT NUMBER

9. SPONSORING / MONITORING AGENCY NAME(S) AND ADDRESS(ES)
U. S. Army Research Office
P.O. Box 12211
Research Triangle Park, NC 27709-2211

10. SPONSORING / MONITORING AGENCY REPORT NUMBER
ARO 35711.26-EG

11. SUPPLEMENTARY NOTES
The views, opinions and/or findings contained in this report are those of the author(s) and should not be construed as an official Department of the Army position, policy or decision, unless so designated by other documentation.

12 a. DISTRIBUTION / AVAILABILITY STATEMENT
Approved for public release; distribution unlimited.

12 b. DISTRIBUTION CODE

13. ABSTRACT
In this investigation, a method for the finite rotation and large deformation analysis of plates is presented. The method, which is based on the absolute nodal coordinate formulation, leads to an isoparametric plate element capable of representing exact rigid body motion. In this method, continuity conditions on all the displacement gradients are imposed. Therefore, non-smoothness of the plate mid-surface at the nodal points is avoided. Unlike other existing finite element formulations that lead to a highly nonlinear inertial forces for three-dimensional elements, the proposed formulation leads to a constant mass matrix, and as a result, the centrifugal and Coriolis forces are identically equal to zero. Furthermore, the method relaxes some of the assumptions used in the classical and Mindlin plate theories. By using a general continuum mechanics approach. a relatively simple expression for the elastic forces is obtained. By developing such an isoparametric plate element. the development of three-dimensional shell elements becomes straightforward. Numerical results are presented in order to demonstrate the use of the proposed method in the large rotating and deformation analysis of plates.

14. SUBJECT TERMS

15. NUMBER OF PAGES

16. PRICE CODE

17. SECURITY CLASSIFICATION OR REPORT	18. SECURITY CLASSIFICATION ON THIS PAGE	19. SECURITY CLASSIFICATION OF ABSTRACT	20. LIMITATION OF ABSTRACT
UNCLASSIFIED	UNCLASSIFIED	UNCLASSIFIED	UL

ABSTRACT

In this investigation, a method for the finite rotation and large deformation analysis of plates is presented. The method, which is based on the absolute nodal coordinate formulation, leads to an isoparametric plate element capable of representing exact rigid body motion. In this method, continuity conditions on all the displacement gradients are imposed. Therefore, non-smoothness of the plate mid-surface at the nodal points is avoided. Unlike other existing finite element formulations that lead to a highly nonlinear inertial forces for three-dimensional elements, the proposed formulation leads to a constant mass matrix, and as a result, the centrifugal and Coriolis forces are identically equal to zero. Furthermore, the method relaxes some of the assumptions used in the classical and Mindlin plate theories. By using a general continuum mechanics approach, a relatively simple expression for the elastic forces is obtained. By developing such an isoparametric plate element, the development of three-dimensional shell elements becomes straightforward. Numerical results are presented in order to demonstrate the use of the proposed method in the large rotating and deformation analysis of plates.

1. INTRODUCTION

Finite element formulations, including incremental methods [1, 2, 10] and large rotation vector formulations [15, 16] are widely and successfully used in the analysis of structural systems. The applications of these formulations to the analysis of large deformation of multibody systems have been a subject of interest in many investigations. The incremental methods lead to a linearization of the rigid body kinematic equations when conventional finite elements are used. In order to overcome this problem, several large rotation vector formulations were recently proposed. In these formulations, finite rotation parameters are used as nodal coordinates. Continuity conditions are imposed on the nodal displacements and the rotation parameters at the element interfaces. The concerns with regard to the use of the large rotation vector formulations in the analysis of flexible multibody systems can be summarized as follows:

1. Imposing continuity on the finite rotations at the nodal points does not guarantee the continuity of the displacement gradients at these points. As a result, the centerline or the mid-surface of the element is not smooth. The obtained solution eventually leads to errors in the calculations of the elastic forces and stresses at the nodal points. This is one of the reasons that most solutions for the large rotation vector formulations are based on incremental procedures and require an elaborate updating scheme for the finite rotation parameters.

2. The interpolation of finite rotations should be carefully handled, particularly in three-dimensional applications. For example, linear interpolation for Euler parameters does not imply linear interpolation for Euler angles [6] or Rodrigues parameters. Different sets of orientation parameters are related by highly nonlinear equations [13]. This fact explains the need to use an accurate updating scheme for the finite rotation parameters in large rotation vector formulations in order to obtain reasonable solutions. In fact, in many of the currently used updating schemes,

an incremental procedure is used by which the finite rotation parameters are incrementally updated to allow exploiting the features of infinitesimal rotations.

3. Most finite element large rotation vector formulations cannot be used to develop a more general beam and plate theory. In the excellent work of Simo [15], a coordinate system is attached to the element cross section. The equations of motion of the cross section, treated as rigid, are developed in terms of a set of generalized coordinates. These generalized coordinates that include finite rotation parameters and depend on the spatial coordinates of the elements are then interpolated using polynomials. By using this procedure, it becomes difficult to relax the assumption of the rigidity of the cross section of the element. This assumption is used in the classical beam and plate theories as well as many of Timoshenko beam [5] and Mindlin plate [8] models.

4. The finite element large rotation vector formulations (as a consequence of 3) do not lead to a constant mass matrix in the case of three-dimensional applications, and as a result, the centrifugal and Coriolis forces are not equal to zero.

Most of these fundamental concerns can be adequately addresses using the absolute nodal coordinate formulation. It is a simple, non-incremental procedure that leads to a constant mass matrix in two- and three-dimensional analysis. It leads to smooth centerline and mid-surface of the elements and ensures the continuity of the rotations of the cross section as well as the displacement gradients at the nodal points. It can also be used to systematically relax some of the assumptions used in Euler-Bernoulli, Timoshenko beam and Mindlin plate models. Furthermore, the absolute nodal coordinate formulation does not require the interpolation of finite rotations and leads to exact modeling of the rigid body dynamics.

One of the features of the non-incremental absolute nodal coordinate formulation is that a global coordinate system is used for the definition of the nodal coordinates. In this case no coordinate transformation is required. The nodal coordinates and the element global shape function are used to define the location and deformation of material points on the finite element. It is, therefore, required that the global shape function must be able to describe the rigid body motion as well as the deformation of the finite element. Another important feature of the formulation is that global slopes instead of angles are used to define the configuration of the finite element. The use of the infinitesimal rotations in the classical finite element formulation, as previously pointed out, leads to linearization of the rigid body kinematic equations, and as a consequence the description of rigid body displacements may not be exact [12]. When global slopes are employed in the absolute nodal coordinate formulation, beam and plate elements become isoparametric while in the classical finite element formulation such elements are considered non-isoparametric.

The objective of this study is to develop a new finite plate element based on the absolute nodal coordinate formulation. In this investigation, a more general plate element is developed by relaxing some of the assumptions of the classical and Mindlin plate theories [17]. The mass matrix of the more general plate element remains constant, and therefore, the centrifugal and Coriolis forces are equal to zero. By using a continuum mechanics approach and nonlinear strain-displacement relationships, a general expression for the elastic forces that takes into account the effect of shear deformation is obtained. Results are presented in this study in order to demonstrate the generality of the new plate model.

2. DISPLACEMENT FIELD

The choice of the type and form of the interpolation functions plays an important role in developing a new type of finite elements. In this study, interpolation polynomial functions are selected because

they are easy to integrate and differentiate. The more complex deformation modes within one element can be achieved by increasing the order of polynomials that define the displacement field of the plate. The use of higher order elements leads to a substantial decrease in the number of elements required to develop a discretized structure model. In the absolute nodal coordinate formulation, the displacement field must include the rigid body modes as well as the plate deformation modes. The following polynomials are assumed to define the displacement field of the plate element used in this investigation:

$$\mathbf{r} = \begin{bmatrix} r_1 \\ r_2 \\ r_3 \end{bmatrix} = \begin{bmatrix} a_0 + a_1x + a_2y + a_3z + a_4xy + a_5xz + a_6yz + a_7x^2 + a_8y^2 + a_9x^2y + a_{10}xy^2 \\ b_0 + b_1x + b_2y + b_3z + b_4xy + b_5xz + b_6yz + b_7x^2 + b_8y^2 + b_9x^2y + b_{10}xy^2 \\ c_0 + c_1x + c_2y + c_3z + c_4xy + c_5xz + c_6yz + c_7x^2 + c_8y^2 + c_9x^2y + c_{10}xy^2 \\ + a_{11}xyz + a_{12}x^3 + a_{13}y^3 + a_{14}x^3y + a_{15}xy^3 \\ + b_{11}xyz + b_{12}x^3 + b_{13}y^3 + b_{14}x^3y + b_{15}xy^3 \\ + c_{11}xyz + c_{12}x^3 + c_{13}y^3 + c_{14}x^3y + c_{15}xy^3 \end{bmatrix}, \tag{1}$$

where $\mathbf{r}$ is the global position vector of an arbitrary point P on the plate, x, y and z are the spatial coordinates of the plate element coordinates and a_i, b_i and c_i are polynomial coefficients that depend on time in the case of dynamic problems. The spatial coordinate z is assumed to be in a direction perpendicular to the mid-surface of the plate in the undeformed state, while the spatial coordinates x and y are measured in the mid-surface plane. The displacement field in the Eq. 1 is expressed in the global coordinate system and therefore the order of the three polynomials are the same. It can be demonstrated using Eq. 1 that the assumed displacement field couples the rigid body motion and the plate deformation. Furthermore, the shear, twist, and rotary inertia effects of the plate are taken into consideration. In Eq. 1, the displacement field depends linearly on the coordinate z since it is assumed that the plate thickness is small compared to the other two dimensions.

3. NODAL COORDINATES AND SHAPE FUNCTIONS

The assumed displacement field of Eq. 1 includes 48 unknown polynomial coefficients, which means that the same number of nodal coordinates is required. Figure 1 shows the element used in this investigation which has nodes *A*, *B*, *C* and *D*. In Fig. 1, *a*, *b*, and *t* are the length, width and thickness of the plate element, respectively. In the model developed in this investigation, 12 coordinates are used for each node. The coordinates $\mathbf{e}_j$ of a node *j* can be chosen as follows:

$$\mathbf{e}_j = \left[\mathbf{r}_j^T \quad \frac{\partial \mathbf{r}_j^T}{\partial x} \quad \frac{\partial \mathbf{r}_j^T}{\partial y} \quad \frac{\partial \mathbf{r}_j^T}{\partial z} \right]^T , \tag{2}$$

where the vector $\mathbf{r}_j$ defines the global position vector of node *j* and the three vectors $\frac{\partial \mathbf{r}_j}{\partial x}$, $\frac{\partial \mathbf{r}_j}{\partial y}$ and $\frac{\partial \mathbf{r}_j}{\partial z}$ define the global displacement gradients of node *j*. Nodal coordinates of one element can then be given by the vector **e**:

$$\mathbf{e} = \left[\mathbf{e}_A^T \quad \mathbf{e}_B^T \quad \mathbf{e}_C^T \quad \mathbf{e}_D^T \right]^T . \tag{3}$$

The polynomial coefficients (a_i, b_i and c_i) can be replaced by the nodal degrees of freedom [11], and the global position vector **r** can be rewritten as follows:

$$\mathbf{r} = \begin{bmatrix} r_1 \\ r_2 \\ r_3 \end{bmatrix} = \mathbf{Se} , \tag{4}$$

where **S** is the matrix of the global shape function. The matrix **S** can be written as:

$$\mathbf{S} = \begin{bmatrix} S_1\mathbf{I} & S_2\mathbf{I} & S_3\mathbf{I} & S_4\mathbf{I} & S_5\mathbf{I} & S_6\mathbf{I} & S_7\mathbf{I} & S_8\mathbf{I} & S_9\mathbf{I} & S_{10}\mathbf{I} \\ S_{11}\mathbf{I} & S_{12}\mathbf{I} & S_{13}\mathbf{I} & S_{14}\mathbf{I} & S_{15}\mathbf{I} & S_{16}\mathbf{I} \end{bmatrix}, \tag{5}$$

where $\mathbf{I}$ is a 3 x 3 identity matrix and

$$S_1 = -(\xi-1)(\eta-1)\left(2\eta^2 - \eta + 2\xi^2 - \xi - 1\right),\ S_2 = -a\xi(\xi-1)^2(\eta-1),$$

$$S_3 = -b\eta(\eta-1)^2(\xi-1),\ S_4 = t\zeta(\xi-1)(\eta-1),\ S_5 = (\eta-1)\xi\left(2\eta^2 - \eta - 3\xi + 2\xi^2\right),$$

$$S_6 = -a\xi^2(\xi-1)(\eta-1),\ S_7 = b\xi\eta(\eta-1)^2,\ S_8 = -t\xi\zeta(\eta-1),$$

$$S_9 = -\xi\eta\left(1 - 3\xi - 3\eta + 2\eta^2 + 2\xi^2\right),\ S_{10} = a\xi^2\eta(\xi-1),\ S_{11} = b\eta^2\xi(\eta-1)$$

$$S_{12} = t\xi\zeta\eta,\ S_{13} = \eta(\xi-1)\left(2\xi^2 - \xi - 3\eta + 2\eta^2\right),\ S_{14} = a\xi\eta(\xi-1)^2$$

$$S_{15} = -b\eta^2(\xi-1)(\eta-1),\ S_{16} = -t\eta\zeta(\xi-1).$$

In the preceding equation, $\xi = x/a$, $\eta = y/b$ and $\zeta = z/t$.

4. RIGID BODY MOTION

If the plate element undergoes an arbitrary rigid body motion, the vectors of nodal coordinates (Eqs. 2 and 3) can be expressed as follows [13]:

$$\mathbf{e}_A = \begin{bmatrix} R_x & R_y & R_z & A_{11} & A_{21} & A_{31} & A_{12} & A_{22} & A_{32} & A_{13} & A_{23} & A_{33} \end{bmatrix}^T,$$

$$\mathbf{e}_B = \begin{bmatrix} R_x + A_{11}a & R_y + A_{21}a & R_z + A_{31}a & A_{11} & A_{21} & A_{31} & A_{12} & A_{22} & A_{32} & A_{13} & A_{23} & A_{33} \end{bmatrix}^T,$$

$$\mathbf{e}_C = \Big[R_x + A_{11}a + A_{12}b \quad R_y + A_{21}a + A_{22}b \quad R_z + A_{31}a + A_{32}b \quad A_{11} \quad A_{21} \quad A_{31} \quad A_{12} \quad A_{22} \quad A_{32} \quad A_{13} \quad A_{23} \quad A_{33} \Big]^T , \tag{6}$$

$$\mathbf{e}_D = \Big[R_x + A_{12}b \quad R_y + A_{22}b \quad R_z + A_{32}b \quad A_{11} \quad A_{21} \quad A_{31} \quad A_{12} \quad A_{22} \quad A_{32} \quad A_{13} \quad A_{23} \quad A_{33} \Big]^T ,$$

where A_{ij} is the ij th element of the 3 x 3 rotation matrix, R_x, R_y and R_z are components of the position vector that defines the global translation of node A of the plate. If rotations are defined in terms of three Euler angles ϕ, θ and ψ, the rotation matrix takes the form:

$$\mathbf{A} = \begin{bmatrix} \cos\psi\cos\phi - \cos\theta\sin\phi\sin\psi & -\sin\psi\cos\phi - \cos\theta\sin\phi\cos\psi & \sin\theta\sin\phi \\ \cos\psi\sin\phi + \cos\theta\cos\phi\sin\psi & -\sin\psi\sin\phi + \cos\theta\cos\phi\cos\psi & -\sin\theta\cos\phi \\ \sin\theta\sin\psi & \sin\theta\cos\psi & \cos\theta \end{bmatrix} . \tag{7}$$

Substituting the expressions of nodal coordinates (Eq. 6) into Eq. 4 that defines the global position vector at an arbitrary point gives:

$$\mathbf{r} = \mathbf{S}\mathbf{e} = \begin{bmatrix} R_x + x(\cos\psi\cos\phi - \cos\theta\sin\phi\sin\psi) - y(\sin\psi\cos\phi + \cos\theta\sin\phi\cos\psi) + z\sin\theta\sin\phi \\ R_y + x(\cos\psi\sin\phi + \cos\theta\cos\phi\sin\psi) + y(\cos\theta\cos\phi\cos\psi - \sin\psi\sin\phi) - z\sin\theta\cos\phi \\ R_z + x\sin\theta\sin\psi + y\sin\theta\cos\psi + z\cos\theta \end{bmatrix} , \tag{8}$$

which demonstrates that an arbitrary rigid body motion can be described using the shape function introduced in Eq. 5. It is clear from the analysis presented in this section that the spatial coordinates x and y represent orthogonal parameterization of the mid plane of the plate in the case of rigid body motion. This is not the case when the plate deforms since in this case $\frac{\partial \mathbf{r}}{\partial x}$ and $\frac{\partial \mathbf{r}}{\partial y}$ do not remain orthogonal.

5. PLATE DEFORMATION

By using global slopes instead of the rotations, no assumptions are made on the magnitude of the rotations within the element. This allows complex shapes to be represented using a small number of elements. As an example, Fig. 2 shows deformed shapes of the plate when one element based on the shape function of Eq. 5 is used. The deformation in Fig. 2a is obtained by using the following numerical values of the nodal coordinates:

$$\mathbf{e} = [0.3\ \ 0.3\ \ -0.2\ \ 1\ \ 0\ \ 1\ \ 0\ \ 0.5\ \ 1\ \ 1\ \ 1\ \ 1\ \ 1\ \ 0\ \ 0\ \ 1\ \ 0\ \ 1\ \ 0\ \ 1\ \ -1\ \ 0\ \ 0\ \ 1$$
$$0.7\ \ 0.7\ \ -0.2\ \ 1\ \ 0\ \ -1\ \ 0\ \ 1\ \ -1\ \ 0\ \ 0\ \ 1\ \ 0\ \ 1\ \ 0\ \ 1\ \ 0\ \ -1\ \ 0\ \ 1\ \ 1\ \ 1\ \ 1\ \ 1]^T \ .$$

The deformation in Fig. 2b is obtained by using the following numerical values of the nodal coordinates:

$$\mathbf{e} = [0.3\ \ 0\ \ 0\ \ 1\ \ 0\ \ 1\ \ 0\ \ 1\ \ 0\ \ 1\ \ 1\ \ 1\ \ 0.7\ \ 0\ \ 0\ \ 1\ \ 0\ \ 1\ \ 0\ \ 1\ \ 0\ \ 0\ \ 1\ \ 1$$
$$1\ \ 1\ \ 0\ \ 1\ \ 0\ \ 1\ \ 0\ \ 1\ \ 0\ \ 0\ \ 0\ \ 1\ \ 0\ \ 1\ \ 0\ \ 1\ \ 0\ \ 1\ \ 0\ \ 1\ \ 0\ \ 1\ \ 1\ \ 1]^T \ .$$

The results presented in Fig. 2 demonstrate that very large deformation and rotation within the plate can be obtained using one element. This important isoparametric property is very crucial in developing efficient shell elements.

In the case of rigid body motion $\frac{\partial \mathbf{r}}{\partial x}$, $\frac{\partial \mathbf{r}}{\partial y}$ and $\frac{\partial \mathbf{r}}{\partial z}$ are three orthogonal unit vectors. This is no longer the case when the plates deforms. Figure 3 shows the norms of these three vectors at points of coordinates $(\xi, \eta, \zeta) = (\xi, 0.5, 0)$ for the deformed plate shown in Fig. 2b. The dot products $\frac{\partial \mathbf{r}}{\partial x} \cdot \frac{\partial \mathbf{r}}{\partial y}$, $\frac{\partial \mathbf{r}}{\partial y} \cdot \frac{\partial \mathbf{r}}{\partial z}$ and $\frac{\partial \mathbf{r}}{\partial x} \cdot \frac{\partial \mathbf{r}}{\partial z}$ are shown in the Fig. 4. The results presented in this figure

show that the three vectors $\frac{\partial \mathbf{r}}{\partial x}$, $\frac{\partial \mathbf{r}}{\partial y}$ and $\frac{\partial \mathbf{r}}{\partial z}$ are, in general, no longer orthogonal vectors when the plate deforms.

The results presented in Figs. 3 and 4 show that the vectors $\frac{\partial \mathbf{r}}{\partial x}$, $\frac{\partial \mathbf{r}}{\partial y}$ and $\frac{\partial \mathbf{r}}{\partial z}$ do not remain orthogonal unit vectors as the plate deforms. The coefficients of the first fundamental form of surfaces can be used to shed light on the configuration of the mid surface as the plate deforms. For the mid surface, $z = 0$ and the first fundamental form in this case is defined as [7]:

$$I = d\mathbf{r}_{z=0} \cdot d\mathbf{r}_{z=0} = E(dx)^2 + 2Fdxdy + G(dy)^2 , \tag{9}$$

where E, F and G are the coefficients of the first fundamental form defined as:

$$E = \left(\frac{\partial \mathbf{r}}{\partial x}\right)^T_{z=0}\left(\frac{\partial \mathbf{r}}{\partial x}\right)_{z=0} , \quad F = \left(\frac{\partial \mathbf{r}}{\partial x}\right)^T_{z=0}\left(\frac{\partial \mathbf{r}}{\partial y}\right)_{z=0} , \quad G = \left(\frac{\partial \mathbf{r}}{\partial y}\right)^T_{z=0}\left(\frac{\partial \mathbf{r}}{\partial y}\right)_{z=0} . \tag{10}$$

The coefficients E and G measure the deviation of $\frac{\partial \mathbf{r}}{\partial x}$ and $\frac{\partial \mathbf{r}}{\partial y}$ from unit vectors. The coefficient F measures the deviation of $\frac{\partial \mathbf{r}}{\partial x}$ and $\frac{\partial \mathbf{r}}{\partial y}$ from orthogonality. Figure 5 shows these three coefficients for the plate shown in Fig. 2b for the spatial coordinates $(\xi, \eta, \zeta) = (\xi, 0.5, 0)$.

6. PLATE INERTIA

In the absolute nodal coordinate formulation, the mass matrix of the plate element can be obtained using the following expression for the kinetic energy:

$$T = \frac{1}{2}\int_V \rho \dot{\mathbf{r}}^T \dot{\mathbf{r}} dV , \tag{11}$$

where ρ is the mass density of the plate, V is the volume and $\dot{\mathbf{r}}$ is the absolute velocity vector. The absolute velocity vector is linear in the nodal velocities and can be obtained by differentiating Eq. 4 with respect to time as follows:

$$\dot{\mathbf{r}} = \mathbf{S}\dot{\mathbf{e}} \quad . \tag{12}$$

Substituting Eq. 12 into the expression of the kinetic energy gives:

$$T = \frac{1}{2}\dot{\mathbf{e}}^T \mathbf{M}\dot{\mathbf{e}} \quad , \tag{13}$$

where $\mathbf{M}$ is the mass matrix given explicitly in the appendix. This mass matrix is constant since it only depends on the inertia properties and dimensions of the plate. As pointed out in previous studies, the mass matrix obtained using the absolute nodal coordinate formulation accounts for the effects rotary inertia and plate twist [9]. As a result of having a constant mass matrix, the centrifugal and Coriolis inertia forces are equal to zero. Having a constant mass matrix allows also the development of an efficient algorithms for solving the nonlinear equations of motion of multibody systems [14, 18].

7. ELASTIC FORCES

The use of a global coordinate system for the definitions of the nodal coordinates leads to a simple expression for the inertia forces and a non-linear expression for the elastic forces. Two different methods can be used when the elastic forces are derived [13]. In one method, a local element coordinate system that is used for the description of the element deformation is introduced. Another method, which is used in this study, is based on a continuum mechanics approach that does not require the use of a local element coordinate system. The latter approach leads to significant simplification in the vector of elastic forces as is previously shown [3]. Furthermore, by employing

a continuum mechanics approach all elastic nonlinearities are taken into consideration since nonlinear strain-displacement relationships must be used.

The elastic forces of the plate element can be derived by using the virtual work or the following expression of the strain energy:

$$U = \frac{1}{2}\int_V \boldsymbol{\varepsilon}_m^T \mathbf{E}\,\boldsymbol{\varepsilon}_m dV \quad , \tag{14}$$

where $\mathbf{E}$ is the matrix of elastic coefficients, and $\boldsymbol{\varepsilon}_m$ is the strain tensor. The strain tensor can be obtained by employing the Cauchy-Green formula [4] as follows:

$$\boldsymbol{\varepsilon}_m = \frac{1}{2}\left(\mathbf{J}^T\mathbf{J} - \mathbf{I}\right) \quad , \tag{15}$$

where $\mathbf{I}$ is a 3 x 3 identity matrix, and $\mathbf{J}$ is the matrix of the displacement gradients. Using Eq. 4 the displacement gradients can be written in the following form:

$$\mathbf{J} = \frac{\partial \mathbf{r}}{\partial \mathbf{x}} = \begin{bmatrix} \frac{\partial \mathbf{S}_1}{\partial x}\mathbf{e} & \frac{\partial \mathbf{S}_1}{\partial y}\mathbf{e} & \frac{\partial \mathbf{S}_1}{\partial z}\mathbf{e} \\ \frac{\partial \mathbf{S}_2}{\partial x}\mathbf{e} & \frac{\partial \mathbf{S}_2}{\partial y}\mathbf{e} & \frac{\partial \mathbf{S}_2}{\partial z}\mathbf{e} \\ \frac{\partial \mathbf{S}_3}{\partial x}\mathbf{e} & \frac{\partial \mathbf{S}_3}{\partial y}\mathbf{e} & \frac{\partial \mathbf{S}_3}{\partial z}\mathbf{e} \end{bmatrix} = \begin{bmatrix} \mathbf{S}_{1x}\mathbf{e} & \mathbf{S}_{1y}\mathbf{e} & \mathbf{S}_{1z}\mathbf{e} \\ \mathbf{S}_{2x}\mathbf{e} & \mathbf{S}_{2y}\mathbf{e} & \mathbf{S}_{2z}\mathbf{e} \\ \mathbf{S}_{3x}\mathbf{e} & \mathbf{S}_{3y}\mathbf{e} & \mathbf{S}_{3z}\mathbf{e} \end{bmatrix} \quad , \tag{16}$$

where $\mathbf{S}_i$ is the ith row of the shape function matrix. The elastic forces of the plate $\mathbf{Q}_k$ can be obtained by differentiating the strain energy once with respect to the nodal coordinates, that is

$$\mathbf{Q}_k = \frac{\partial U}{\partial \mathbf{e}} \quad . \tag{17}$$

It can be shown that the shape function (of Eq. 5) leads to zero elastic forces under an arbitrary rigid body displacement. The vector of the elastic forces can also be expressed as a product of a nonlinear stiffness matrix **K** and the vector of nodal coordinates **e** as follows:

$$\mathbf{Q}_k = \mathbf{K}\mathbf{e} \quad . \tag{18}$$

It can be shown that the stiffness matrix of the plate element can be written as follows:

$$\mathbf{K} = \mathbf{K}_1 + \mathbf{K}_2 + \mathbf{K}_3 + \mathbf{K}_4 + \mathbf{K}_5 + \mathbf{K}_6 \quad , \tag{19}$$

where

$$\mathbf{K}_1 = \frac{1}{8}\int_V \mathbf{b}_2^T\left[\lambda\left(\mathbf{e}^T\mathbf{b}_1\mathbf{e}-1\right)+(\lambda+2\mu)\left(\mathbf{e}^T\mathbf{b}_2\mathbf{e}-1\right)+\lambda\left(\mathbf{e}^T\mathbf{b}_3\mathbf{e}-1\right)\right]+ \left(\mathbf{e}^T\mathbf{b}_2^T\mathbf{e}-1\right)\left(\lambda\mathbf{b}_1+(\lambda+2\mu)\mathbf{b}_2+\lambda\mathbf{b}_3\right)dV \quad ,$$

$$\mathbf{K}_2 = \frac{1}{8}\int_V \mathbf{b}_3^T\left[\lambda\left(\mathbf{e}^T\mathbf{b}_2\mathbf{e}-1\right)+(\lambda+2\mu)\left(\mathbf{e}^T\mathbf{b}_3\mathbf{e}-1\right)+\lambda\left(\mathbf{e}^T\mathbf{b}_1\mathbf{e}-1\right)\right]+ \left(\mathbf{e}^T\mathbf{b}_3^T\mathbf{e}-1\right)\left(\lambda\mathbf{b}_2+(\lambda+2\mu)\mathbf{b}_3+\lambda\mathbf{b}_1\right)dV \quad ,$$

$$\mathbf{K}_3 = \frac{1}{8}\int_V \mathbf{b}_1^T\left[\lambda\left(\mathbf{e}^T\mathbf{b}_2\mathbf{e}-1\right)+(\lambda+2\mu)\left(\mathbf{e}^T\mathbf{b}_1\mathbf{e}-1\right)+\lambda\left(\mathbf{e}^T\mathbf{b}_3\mathbf{e}-1\right)\right]+ \left(\mathbf{e}^T\mathbf{b}_1^T\mathbf{e}-1\right)\left(\lambda\mathbf{b}_2+(\lambda+2\mu)\mathbf{b}_1+\lambda\mathbf{b}_3\right)dV \quad ,$$

$$\mathbf{K}_4 = \frac{1}{4}\mu\int_V \mathbf{b}_4^T\cdot\mathbf{e}^T\mathbf{b}_4\mathbf{e}+\mathbf{e}^T\mathbf{b}_4^T\mathbf{e}\cdot\mathbf{b}_4\,dV\,,\quad \mathbf{K}_5 = \frac{1}{4}\mu\int_V \mathbf{b}_5^T\cdot\mathbf{e}^T\mathbf{b}_5\mathbf{e}+\mathbf{e}^T\mathbf{b}_5^T\mathbf{e}\cdot\mathbf{b}_5\,dV\,,$$

$$\mathbf{K}_6 = \frac{1}{4}\mu\int_V \mathbf{b}_6^T\cdot\mathbf{e}^T\mathbf{b}_6\mathbf{e}+\mathbf{e}^T\mathbf{b}_6^T\mathbf{e}\cdot\mathbf{b}_6\,dV\,,$$

where μ and λ are Lame's constant, and

$$\mathbf{b}_1 = \mathbf{S}_{3x}^T \mathbf{S}_{1z} + \mathbf{S}_{3y}^T \mathbf{S}_{2z} + \mathbf{S}_{3z}^T \mathbf{S}_{3z}, \qquad \mathbf{b}_2 = \mathbf{S}_{1x}^T \mathbf{S}_{1x} + \mathbf{S}_{1y}^T \mathbf{S}_{2x} + \mathbf{S}_{1z}^T \mathbf{S}_{3x},$$

$$\mathbf{b}_3 = \mathbf{S}_{2x}^T \mathbf{S}_{1y} + \mathbf{S}_{2y}^T \mathbf{S}_{2y} + \mathbf{S}_{2z}^T \mathbf{S}_{3y}, \qquad \mathbf{b}_4 = \mathbf{S}_{1x}^T \mathbf{S}_{1y} + \mathbf{S}_{1y}^T \mathbf{S}_{2y} + \mathbf{S}_{1z}^T \mathbf{S}_{3y},$$

$$\mathbf{b}_5 = \mathbf{S}_{1x}^T \mathbf{S}_{1z} + \mathbf{S}_{1y}^T \mathbf{S}_{2z} + \mathbf{S}_{1z}^T \mathbf{S}_{3z}, \qquad \mathbf{b}_6 = \mathbf{S}_{2x}^T \mathbf{S}_{1z} + \mathbf{S}_{2y}^T \mathbf{S}_{2z} + \mathbf{S}_{2z}^T \mathbf{S}_{3z}.$$

8. IMPLEMENTATION AND NUMERICAL RESULTS

The use of the new plate element developed in this study is demonstrated in this section by studying the behavior of two simple pendulums. Using the developments presented in the preceding sections, the equations of motion of the finite element can be written in a matrix form as follows [13]:

$$\mathbf{M}\ddot{\mathbf{e}} + \mathbf{K}\mathbf{e} = \mathbf{Q}_e \quad , \tag{20}$$

where $\mathbf{Q}_e$ is the vector of the generalized external nodal forces. Using the definition of the elastic forces, the preceding equation can be written as:

$$\mathbf{M}\ddot{\mathbf{e}} = \mathbf{Q} \quad , \tag{21}$$

where the force vector $\mathbf{Q}$ is given by

$$\mathbf{Q} = \mathbf{Q}_e - \mathbf{Q}_k \quad . \tag{22}$$

Since the mass matrix is constant the equation of motion can be efficiently solved for the accelerations using the following equation:

$$\ddot{\mathbf{e}} = \mathbf{M}^{-1}\mathbf{Q} \quad . \tag{23}$$

The pendulum plate models in this investigation are shown in Fig. 6. One plate model has one element, while the other model has three elements. In the two models, the plate is connected to the ground using a spherical joint. Therefore, each model has three rigid body rotational degrees of freedom. The two pendulums are assumed to vibrate under the effect of gravity. The length, width and thickness of the first plate are 0.3 m, 0.3 m, and 0.01 m, respectively. The material of the plate is assumed to be isotropic and its Young's modulus is $1.0 \cdot 10^5$ N/m^2, Poisson's ration is 0.3 and mass density is 7810 kg/m^3. Figure 7 shows the motion simulation of the first pendulum and Fig. 8 shows the global coordinates of point H (Fig. 6) versus time. As shown in the Fig. 7, one element is capable of representing large deformation and rotation of the flexible plate under the effect of gravity.

The second pendulum model has a rectangular plate that has length, width and thickness of 0.3 m, 0.6 m, and 0.01 m, respectively. The material properties of the plate in this model are assumed to be the same as the properties used in the first model. Figure 9 shows the simulation of the plate motion under the effect of gravity. Figure 10 shows the global coordinates of point H (Fig. 6) of the pendulum versus time. The components of the vectors $\frac{\partial \mathbf{r}}{\partial x}$, $\frac{\partial \mathbf{r}}{\partial y}$ and $\frac{\partial \mathbf{r}}{\partial z}$ along line I (Fig. 6) on the mid surface of the plate at time 1.1 s are shown in Figs. 11, 12 and 13. The results presented in these figures demonstrate that the global displacement gradients at the nodal points are continuous.

9. SUMMARY AND CONCLUSIONS

In this investigation, a new plate element developed using the non-incremental absolute nodal coordinate formulation is presented. The general plate model developed in this investigation can

describe rigid body motion, finite rotations and an arbitrary large deformation. Continuity of all displacement gradients at the element nodal points are ensured, thereby, ensuring the smoothness of the mid-surface of the plate structures at the element nodes. While the plate element developed in this study relaxes some of the assumptions of the conventional and Mindlin plate theories, the mass matrix remains constant when the plate undergoes finite rotations and experiences large deformation. It is demonstrated in this investigation that complex deformation shapes can be modeled using small number of elements. By using global slopes instead of rotations, no assumptions are made with regard to the magnitude of the rotations or the deformation within the element. A continuum mechanics approach is used to obtain the plate elastic forces. Nonlinear strain –displacement relationship are used in formulating the elastic forces and as a result the formulation presented in this paper accounts for all geometric nonlinearities. The plate element developed in this study is of the isoparametric type and can be used to develop efficient shell formulations.

APPENDIX

The mass matrix **M** in Eq. 13 is defined as follows:

$$\mathbf{M} = \begin{bmatrix} \mathbf{M}_{aa} & \mathbf{M}_{ab} \\ symm. & \mathbf{M}_{bb} \end{bmatrix}$$

The submatrises $\mathbf{M}_{aa}$, $\mathbf{M}_{ab}$ and $\mathbf{M}_{bb}$ can be written as:

$\mathbf{M}_{aa} =$

$$\begin{bmatrix}
\frac{1727}{12600}m\mathbf{I} & \frac{461}{25200}bm\mathbf{I} & \frac{461}{12600}\rho bQ_z\mathbf{I} & \frac{11}{90}\rho bQ_y\mathbf{I} & \frac{613}{12600}m\mathbf{I} & -\frac{137}{12600}bm\mathbf{I} & \frac{199}{12600}\rho bQ_z\mathbf{I} & \frac{19}{360}\rho bQ_y\mathbf{I} \\
 & \frac{1}{315}b^2m\mathbf{I} & \frac{1}{200}\rho b^2Q_z\mathbf{I} & \frac{1}{60}\rho b^2Q_y\mathbf{I} & \frac{137}{12600}bm\mathbf{I} & -\frac{1}{420}b^2m\mathbf{I} & \frac{1}{300}\rho b^2Q_z\mathbf{I} & \frac{1}{90}\rho b^2Q_y\mathbf{I} \\
 & & \frac{1}{105}\rho bI_{zz}\mathbf{I} & \frac{1}{30}\rho bI_{yz}\mathbf{I} & \frac{199}{12600}\rho bQ_z\mathbf{I} & -\frac{1}{300}\rho b^2Q_z\mathbf{I} & \frac{1}{210}\rho b^2I_{zz}\mathbf{I} & \frac{1}{60}\rho bI_{yz}\mathbf{I} \\
 & & & \frac{1}{9}\rho bI_{yy}\mathbf{I} & \frac{19}{360}\rho bQ_y\mathbf{I} & -\frac{1}{90}\rho b^2Q_y\mathbf{I} & \frac{1}{60}\rho bI_{yz}\mathbf{I} & \frac{1}{18}\rho bI_{yy}\mathbf{I} \\
 & & & & \frac{1727}{12600}m\mathbf{I} & -\frac{461}{25200}bm\mathbf{I} & \frac{461}{12600}\rho bQ_z\mathbf{I} & \frac{11}{90}\rho bQ_y\mathbf{I} \\
 & & & & & \frac{1}{315}b^2m\mathbf{I} & -\frac{1}{200}\rho b^2Q_z\mathbf{I} & -\frac{1}{60}\rho b^2I_{yz}\mathbf{I} \\
 & symm. & & & & & \frac{1}{105}\rho bI_{zz}\mathbf{I} & \frac{1}{30}\rho bI_{yz}\mathbf{I} \\
 & & & & & & & \frac{1}{9}\rho bI_{yy}\mathbf{I}
\end{bmatrix},$$

$\mathbf{M}_{ab} =$

$$\begin{bmatrix}
\frac{197}{12600}m\mathbf{I} & -\frac{29}{6300}bm\mathbf{I} & -\frac{29}{3150}\rho bQ_z\mathbf{I} & \frac{1}{45}\rho bQ_y\mathbf{I} & \frac{613}{12600}m\mathbf{I} & \frac{199}{25200}bm\mathbf{I} & -\frac{137}{6300}\rho bQ_z\mathbf{I} & \frac{19}{360}\rho bQ_y\mathbf{I} \\
\frac{29}{6300}bm\mathbf{I} & -\frac{1}{840}b^2m\mathbf{I} & -\frac{1}{450}\rho b^2Q_z\mathbf{I} & \frac{1}{180}\rho b^2Q_y\mathbf{I} & \frac{199}{25200}bm\mathbf{I} & \frac{1}{630}b^2m\mathbf{I} & -\frac{1}{300}\rho b^2Q_z\mathbf{I} & \frac{1}{120}\rho b^2Q_y\mathbf{I} \\
\frac{29}{3150}\rho bQ_z\mathbf{I} & -\frac{1}{450}\rho b^2Q_z\mathbf{I} & -\frac{1}{280}\rho bI_{zz}\mathbf{I} & \frac{1}{90}\rho bI_{yz}\mathbf{I} & \frac{137}{6300}\rho bQ_z\mathbf{I} & \frac{1}{300}\rho b^2Q_z\mathbf{I} & -\frac{1}{140}\rho b^2I_{zz}\mathbf{I} & \frac{1}{45}\rho bI_{yz}\mathbf{I} \\
\frac{1}{45}\rho bQ_y\mathbf{I} & -\frac{1}{180}\rho b^2Q_y\mathbf{I} & -\frac{1}{90}\rho bI_{yz}\mathbf{I} & \frac{1}{36}\rho bI_{yy}\mathbf{I} & \frac{19}{360}\rho bQ_y\mathbf{I} & \frac{1}{120}\rho b^2Q_y\mathbf{I} & -\frac{1}{45}\rho bI_{yz}\mathbf{I} & \frac{1}{18}\rho bI_{yy}\mathbf{I} \\
\frac{613}{12600}m\mathbf{I} & -\frac{199}{25200}bm\mathbf{I} & -\frac{137}{6300}\rho bQ_z\mathbf{I} & \frac{19}{360}\rho bQ_y\mathbf{I} & \frac{197}{12600}m\mathbf{I} & \frac{29}{6300}bm\mathbf{I} & -\frac{29}{3150}\rho bQ_z\mathbf{I} & \frac{1}{45}\rho bQ_y\mathbf{I} \\
-\frac{199}{25200}bm\mathbf{I} & \frac{1}{630}b^2m\mathbf{I} & \frac{1}{300}\rho b^2Q_z\mathbf{I} & -\frac{1}{120}\rho b^2Q_y\mathbf{I} & -\frac{29}{6300}bm\mathbf{I} & -\frac{1}{840}b^2m\mathbf{I} & \frac{1}{450}\rho b^2Q_z\mathbf{I} & -\frac{1}{180}\rho b^2I_{yz}\mathbf{I} \\
\frac{137}{6300}\rho bQ_z\mathbf{I} & -\frac{1}{300}\rho b^2Q_z\mathbf{I} & -\frac{1}{140}\rho b^2I_{zz}\mathbf{I} & \frac{1}{45}\rho bI_{yz}\mathbf{I} & \frac{29}{3150}\rho bQ_z\mathbf{I} & \frac{1}{450}\rho b^2Q_z\mathbf{I} & \frac{1}{280}\rho bI_{zz}\mathbf{I} & \frac{1}{90}\rho bI_{yz}\mathbf{I} \\
\frac{19}{360}\rho bQ_y\mathbf{I} & -\frac{1}{120}\rho b^2Q_y\mathbf{I} & -\frac{1}{45}\rho bI_{yz}\mathbf{I} & \frac{1}{18}\rho bI_{yy}\mathbf{I} & \frac{1}{45}\rho bQ_y\mathbf{I} & \frac{1}{180}\rho b^2I_{yz}\mathbf{I} & -\frac{1}{90}\rho bI_{yz}\mathbf{I} & \frac{1}{36}\rho bI_{yy}\mathbf{I}
\end{bmatrix}.$$

$$\mathbf{M}_{bb} =$$

$$\begin{bmatrix}
\frac{1727}{12600}m\mathbf{I} & -\frac{461}{25200}bm\mathbf{I} & -\frac{461}{12600}\rho bQ_z\mathbf{I} & \frac{11}{90}\rho bQ_y\mathbf{I} & \frac{613}{12600}m\mathbf{I} & \frac{137}{12600}bm\mathbf{I} & -\frac{199}{12600}\rho bQ_z\mathbf{I} & \frac{19}{360}\rho bQ_y\mathbf{I} \\
 & \frac{1}{315}b^2m\mathbf{I} & \frac{1}{200}\rho b^2Q_z\mathbf{I} & -\frac{1}{60}\rho b^2Q_y\mathbf{I} & -\frac{137}{12600}bm\mathbf{I} & -\frac{1}{420}b^2m\mathbf{I} & \frac{1}{300}\rho b^2Q_z\mathbf{I} & -\frac{1}{90}\rho b^2Q_y\mathbf{I} \\
 & & \frac{1}{105}\rho bI_{zz}\mathbf{I} & -\frac{1}{30}\rho bI_{yz}\mathbf{I} & -\frac{199}{12600}\rho bQ_z\mathbf{I} & -\frac{1}{300}\rho b^2Q_z\mathbf{I} & \frac{1}{210}\rho b^2I_{zz}\mathbf{I} & -\frac{1}{60}\rho bI_{yz}\mathbf{I} \\
 & & & \frac{1}{9}\rho bI_{yy}\mathbf{I} & \frac{19}{360}\rho bQ_y\mathbf{I} & \frac{1}{90}\rho b^2Q_y\mathbf{I} & -\frac{1}{60}\rho bI_{yz}\mathbf{I} & \frac{1}{18}\rho bI_{yy}\mathbf{I} \\
 & & & & \frac{1727}{12600}m\mathbf{I} & \frac{461}{25200}bm\mathbf{I} & -\frac{461}{12600}\rho bQ_z\mathbf{I} & \frac{11}{90}\rho bQ_y\mathbf{I} \\
 & & & & & \frac{1}{315}b^2m\mathbf{I} & \frac{1}{200}\rho b^2Q_z\mathbf{I} & \frac{1}{60}\rho b^2I_{yz}\mathbf{I} \\
 & \textit{symm.} & & & & & \frac{1}{105}\rho bI_{zz}\mathbf{I} & -\frac{1}{30}\rho bI_{yz}\mathbf{I} \\
 & & & & & & & \frac{1}{9}\rho bI_{yy}\mathbf{I}
\end{bmatrix},$$

where $\mathbf{I}$ is a 3x3 identity matrix, m is the element mass and ρ is the mass density of the element and

$$Q_y = \frac{1}{2}at^2, \quad Q_z = \frac{1}{2}a^2t, \quad I_{yy} = \frac{1}{3}at^3, \quad I_{zz} = \frac{1}{3}a^3t, \quad I_{yz} = \frac{1}{4}a^2t^2.$$

Acknowledgment

This study was supported by the Academy of Finland and, in part, by the National Science Foundation and the U.S. Army Research Office, Research Triangle Park, N.C.

REFERENCES

[1] *ANSYS User's Manual*, 1997, Theory, Ninth Edition, SAS IP, Inc.

[2] Belytschko, T. and Hsieh, B.J., 1973, "Nonlinear Transient Finite Element Analysis with Convected Coordinates," *International Journal for Numerical Methods in Engineering*, **7**, pp. 255-271.

[3] Berzeri, M. and Shabana, A.A., 2000, "Development of Simple Models for the Elastic Forces in the Absolute Nodal Co-ordinate Formulation," *Journal of Sound and Vibration*, **235**(4), pp. 539-565.

[4] Bonet, J. and Wood, R.D., 1997, "*Nonlinear Continuum Mechanics for Finite Element Analysis*," Cambridge University Press, Campridge.

[5] Dym, C.L. and Shames, I.H., 1973, "*Solid Mechanics, a Variational Approach*," McGraw-Hill.

[6] Goldstein, H., 1951,"*Classical mechanics*", Addison-Wesley.

[7] Lass, H., 1950," *Vector and Tensor Analysis*," McGraw-Hill.

[8] Mindlin, R.D., 1951, "Influence of Rotary Inertia and Shear on Flexural motions of Isotropic, Elastic Plates," *ASME Journal of Applied Mechanics*, **18**, pp. 31-38.

[9] Omar, M.A. and Shabana, A.A., "Development of a Shear Deformable Element Using the Absolute Nodal Coordinate Formulation," *Technical Report MBS00-3-UIC*, University of Illinois at Chicago, Chicago, IL.

[10] Rankin, C.C. and Brogan, F.A., 1986, "An Element Independent Corotational Procedure for the Treatment of Large Rotations," *ASME Journal of Pressure Vessel Technology*, **108**, pp. 165-174.

[11] Rao, S.S., 1982, "*The Finite Element Method in Engineering*," Pergamon Press.

[12] Shabana, A.A., 1996, "Finite Element Incremental Approach and Exact Rigid Body Inertia," *Journal of Mechanical Design*, **118**, pp. 171-178.10

[13] Shabana A.A., 1998, "*Dynamics of Multibody Systems, 2nd edition*," Cambridge University Press.

[14] Shabana, A.A., 1998, "Computer Implementation of the Absolute Nodal Coordinate Formulation for Flexible Multibody Dynamics," *Nonlinear dynamics*, **16**, pp. 293-306.

[15] Simo, J.C. and Vu-Quoc, L., 1986, "On the Dynamics of Flexible Beams Under Large Overall Motion – the Plane Case: Part I, " *ASME Journal of Applied Mechanics*, **53**, pp. 849-854.

[16] Simo, J.C., 1986, "A Three-Dimensional Finite-Strain Rod Model. Part II: Computational Aspects," *Journal of Computer Method in Applied Mechanics and Engineering*, **58**, pp. 79-116.

[17] Stanley, G.M., Park, K.C. and Hughes, T.J.R., 1986, "Continuum-Based Resultant Shell Elements," in *Finite Element Methods for Plate and Shell Structures. Volume 1: Element Technology*, Hughes, T.J.R. and Hinton, E., Pineridge Press International, pp. 1-45.

[18] Yakoub, R.Y. and Shabana, A.A., 1999, "Use of Cholesky Coordinates and the Absolute Nodal Coordinate Formulation in the Computer Simulation of Flexible Multibody Systems," *Journal of Nonlinear Dynamics*, **20**, pp. 267-282.

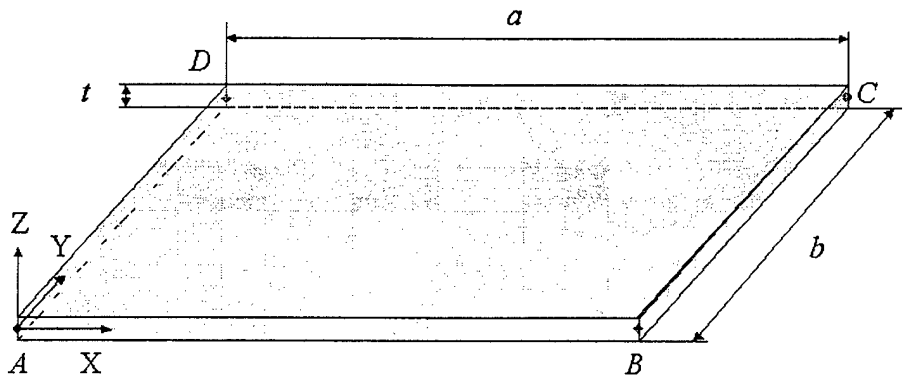

Fig. 1. The four node plate element.

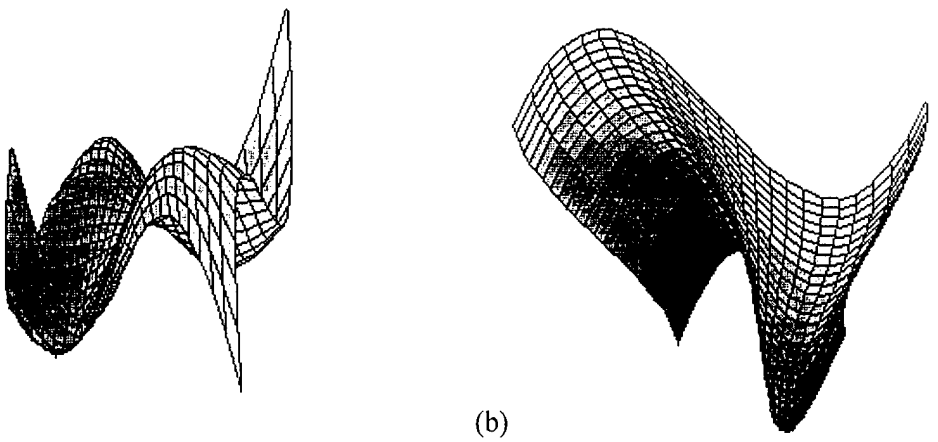

Fig. 2. Examples of plate deformations.

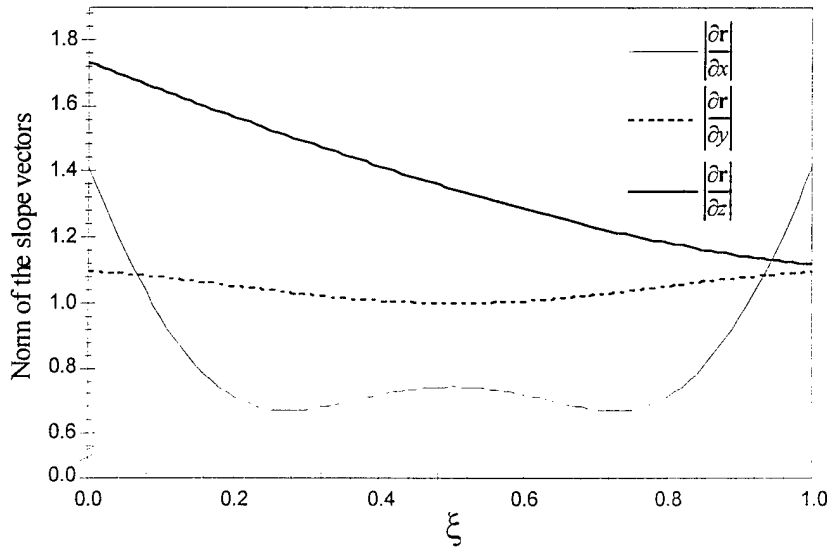

Fig. 3. Norms of vectors $\frac{\partial \mathbf{r}}{\partial x}$, $\frac{\partial \mathbf{r}}{\partial y}$ and $\frac{\partial \mathbf{r}}{\partial z}$.

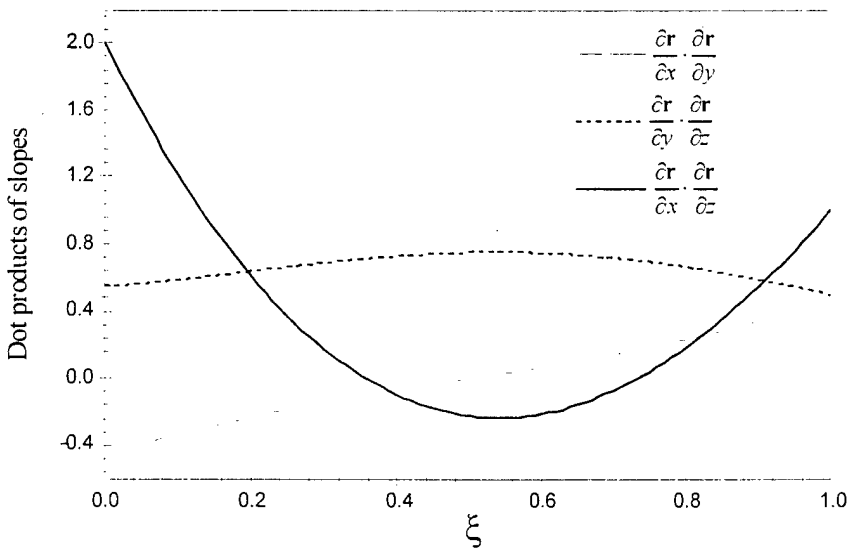

Fig. 4. Dot products $\frac{\partial \mathbf{r}}{\partial x} \cdot \frac{\partial \mathbf{r}}{\partial y}$, $\frac{\partial \mathbf{r}}{\partial y} \cdot \frac{\partial \mathbf{r}}{\partial z}$ and $\frac{\partial \mathbf{r}}{\partial x} \cdot \frac{\partial \mathbf{r}}{\partial z}$.

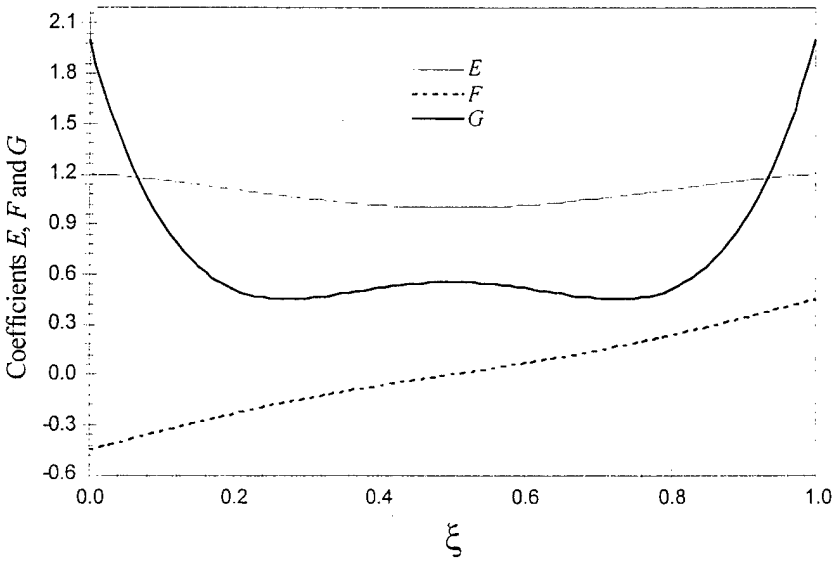

Fig. 5. The coefficients E, F and G.

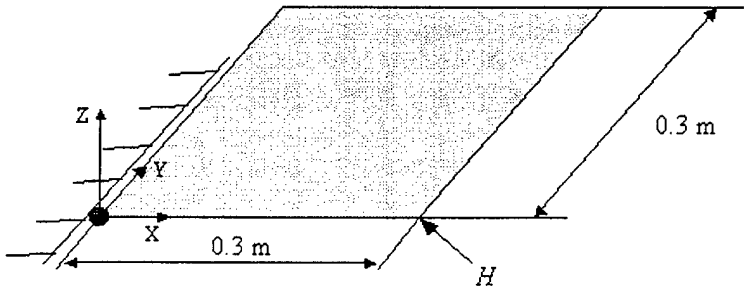

First pendulum

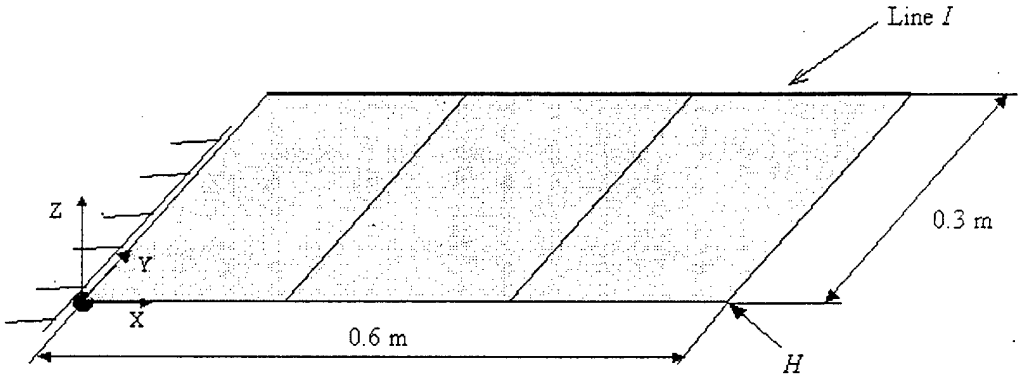

Second pendulum

Fig. 6. Pendulum models.

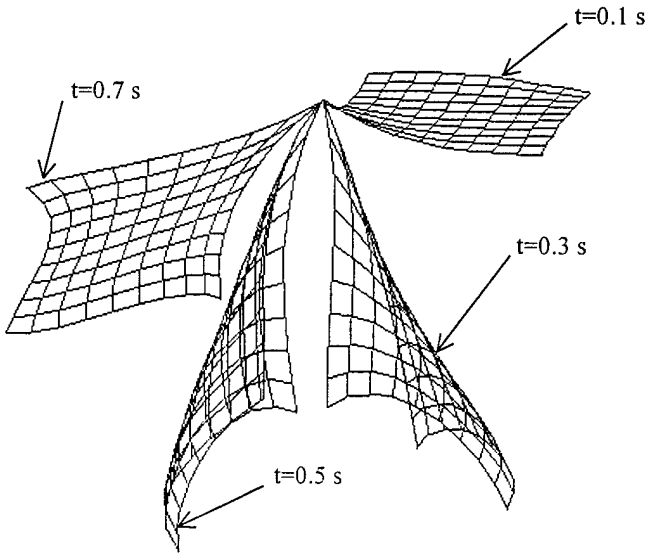

Fig. 7. Motion simulation of the first plate model.

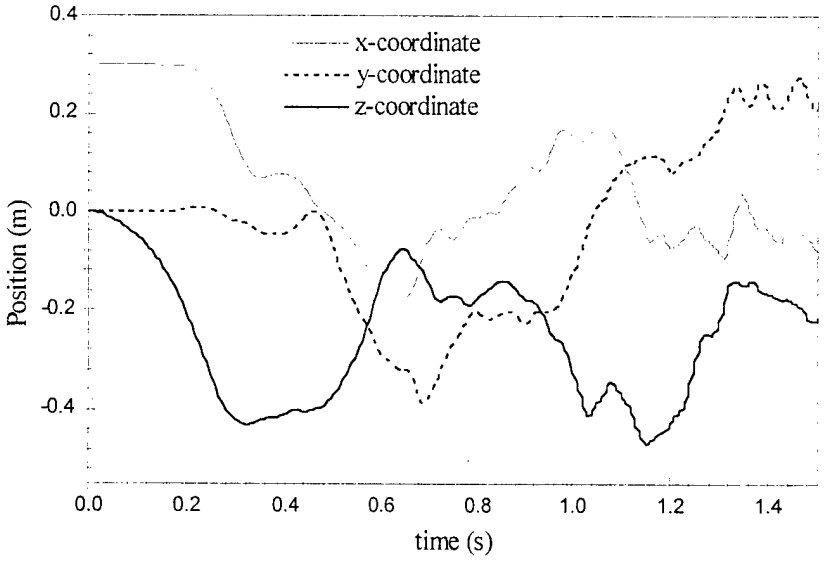

Fig. 8. Global coordinates of point *H* of the first pendulum.

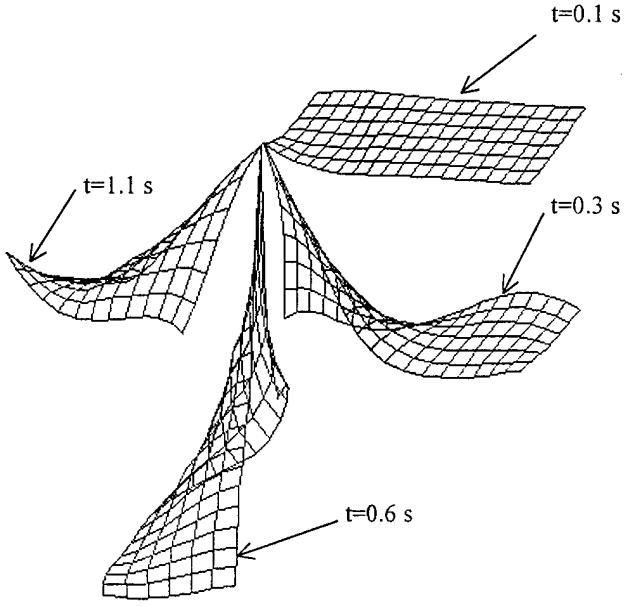

Fig. 9. Configurations of the second plate model.

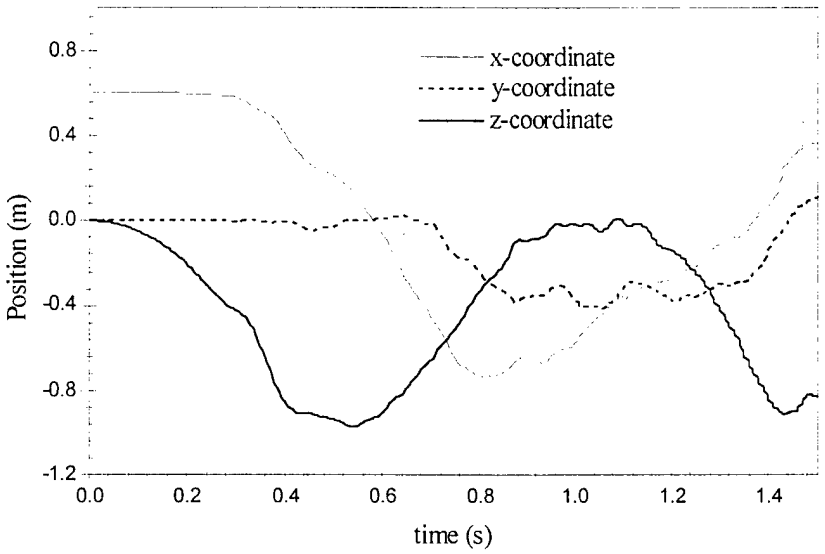

Fig. 10. Global coordinates of the free end (point *H*) of the second pendulum.

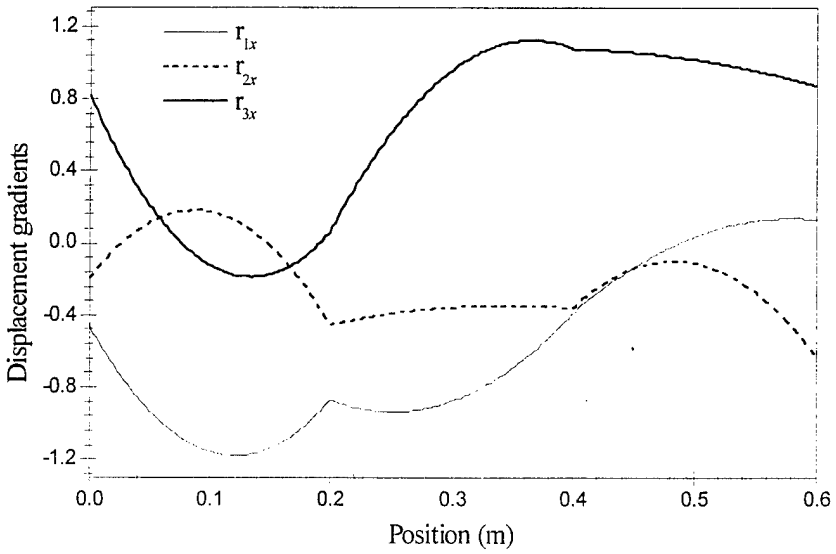

Fig. 11. Components of the vector $\frac{\partial \mathbf{r}}{\partial x}$.

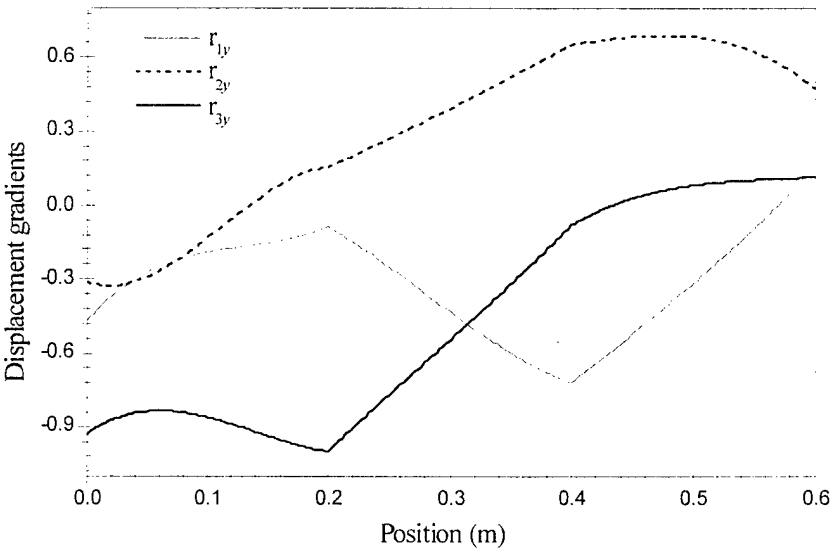

Fig. 12. Components of the vector $\frac{\partial \mathbf{r}}{\partial y}$.

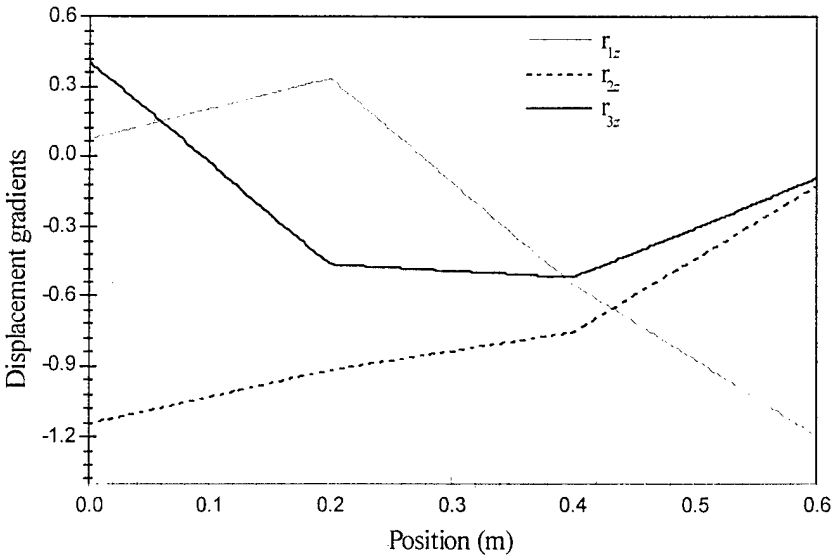

Fig. 13. Components of the vector $\frac{\partial \mathbf{r}}{\partial z}$.